

# DYNAMIC INSTABILITY CHARACTERISTICS OF ROLLING ELEMENT BEARINGS

Sreedath Panat, Baldev Puliyeri, Srinath Ramagiri and Abhijit Sarkar

*Indian Institute of Technology Madras, Department of Mechanical Engineering, Chennai, India*  
email: [asarkar@iitm.ac.in](mailto:asarkar@iitm.ac.in)

The dynamics of bearing is a classical problem in machinery vibration. It is well known that rolling element bearings are susceptible to large vibration response at suitable parameter values arising due to instability. In the present work, we formulate the governing equations of motion of rolling element bearings. Herein, the rolling elements are modeled as lumped spring elements. With odd number of rolling elements, due to asymmetric effects of the bearing cross-section a parametric excitation effect is introduced in the system of governing equations. Further, due to the load zone effect this system represents a non-smooth dynamical system. The parametric stiffness term flips its sign depending on the sign of the displacement response. As such the governing equations of the system resemble the classical asymmetric Mathieu equation. In the literature, the method of Lyapunov-like exponents has been used to determine the stability boundaries of the asymmetric Mathieu equation. Herein, a positive Lyapunov-like exponent indicates instability whereas a stable response manifests as a negative Lyapunov-like exponent. In the present work, we use this method in detecting the stability and instability characteristics over the different bearing parameters. Stability diagrams are presented which can aid the designers and the user of the bearing in confirming the stability and instability zone. The method is validated by numerically integrating the governing equations. It is verified through numerical analysis that parameter combinations associated with an unstable zone manifest an exponential growth in response. Similarly, the parameter combinations associated with stable zone of the stability diagram shows bounded response.

Keywords: Bearing, Mathieu equation, parametric excitation

---

## 1. Introduction

The dynamic instability characteristic of bearings is a problem of interest for both industry and academia. Despite being a well-developed topic, there are certain aspects of bearing vibration that have not been investigated thoroughly. The vibration in rolling element bearings due to parametric excitation is one such area. As the bearing rotates, the configuration of rolling elements between the inner and outer race continuously change, thereby leading to a periodic variation of the effective stiffness of the bearing assembly. This dynamic stiffness is responsible for the parametrically excited vibration. However in case of bearings with odd number of rolling elements, the stiffness of the bearing becomes asymmetric, thereby making the analysis complicated. This work aims to throw light into the stability characteristics of parametrically excited vibration in bearings with odd number of rolling elements.

The effect of number of balls and pre-load on bearing vibration was studied by Aktürk et. al. [1]. The dynamic effects of varying compliance in bearings has been investigated by Walters [2] using motion simulation but without the effect of geometry of the rolling elements taken into consideration. A dynamic model for both ball and cylindrical roller bearings was later developed by Gupta [3] with the assumption of non-linear Hertzian contact stiffness. Estimation of static stiffness parameters was done by Shimizu et. al. [4] and overall stiffness was found to be changing with dif-

ferent positions of the rolling elements. Thus natural frequency of the system in various configurations changes over a full cycle of rotation. Analysis based on Floquet theory is a classical method of solution for such parametrically excited system as done by Nayfeh et. al. [5].

Srinath et.al. [6] studied the parametrically excited vibration in rolling element bearing by formulating governing equations of motion into 2-DOF coupled Mathieu equations. Floquet theory was used for determining the instability. But the asymmetry involved in Mathieu equation was not taken into consideration owing to the complexity involved in its solution. Marathe et.al. [7] studied the parametric instability in single degree of freedom systems (inverted pendulum) with asymmetric stiffness condition using Lyapunov-like exponent.

The current work aims to predict the stable and unstable operational ranges of speed for a particular rolling element bearing configuration by numerically solving the governing two dimensional coupled asymmetric Mathieu equation and evaluating the value of a Lyapunov-like exponent. The inclusion of asymmetry in the analysis makes the study closer to reality than previous works on this problem.

## 2. Formulation

A typical rolling element bearing comprises of inner and outer race,  $n$  rolling elements and cage. The races are assumed to be rigidly connected to separate machine elements, and the rolling elements to be elastic with a stiffness value. Zero clearance is assumed between the rollers and races, which leads to a load zone of  $180^\circ$  as shown in Fig. 1(a). The load is transferred between the races through the rolling elements within the load zone. Roller bearings are modelled as individual springs as shown in Fig. 1(b) and hence the system is modelled as a spring-mass system with two degrees of freedom as in Fig. 1(c). Newton's second law applied to this system gives the equation of motion as shown in Eq. (1).

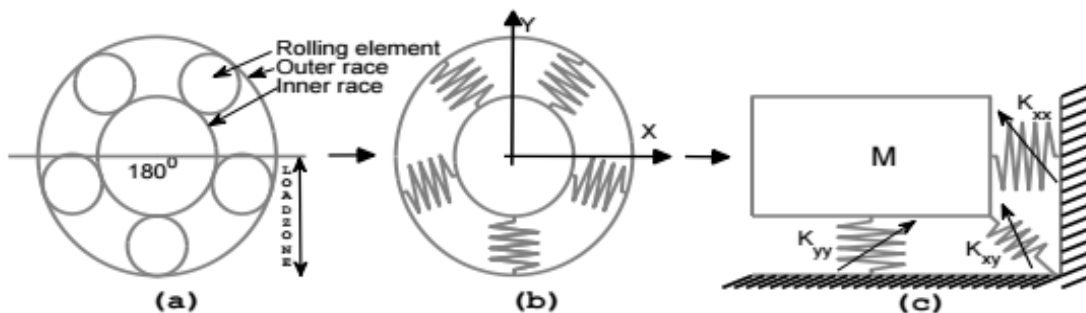


Figure 1: (a) Bearing load zone (b) Spring modelling (c) Spring mass system

$$[M] \begin{Bmatrix} \ddot{x} \\ \ddot{y} \end{Bmatrix} + [K(t)] \begin{Bmatrix} x \\ y \end{Bmatrix} = 0 \quad (1)$$

Where  $[M]$  is the mass matrix and  $[K(t)]$  is the dynamic stiffness matrix of the bearing system. Calculation of  $[K(t)]$  has been done by Srinath et. al [6]. The static stiffness values of individual rolling elements were evaluated using finite element simulations in ANSYS 13.0 by applying vertical load and measuring the compression. To measure the static stiffness of the bearing system, horizontal and vertical loads were applied in the positive  $x$  and  $y$  direction respectively and the corresponding deflections were measured. The ratio of vertical reaction and vertical displacement gave static direct stiffness and ratio of horizontal reaction and vertical deflection gave static cross-coupled stiffness. As the bearing rotates the number of rolling elements and their configuration within the load zone changes. This leads to time varying stiffness as shown in Fig. 2. This variation of stiffness as the bearing rotates was expanded into a Fourier series. Taking only the dominant harmonics in the Fourier series expansion, dynamic stiffness matrix  $[K(t)]$  can be expressed as per Eq. (2).

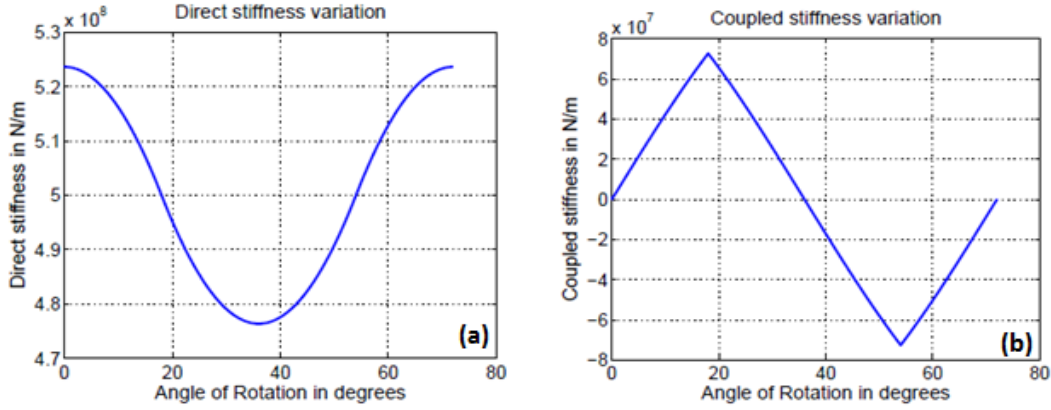
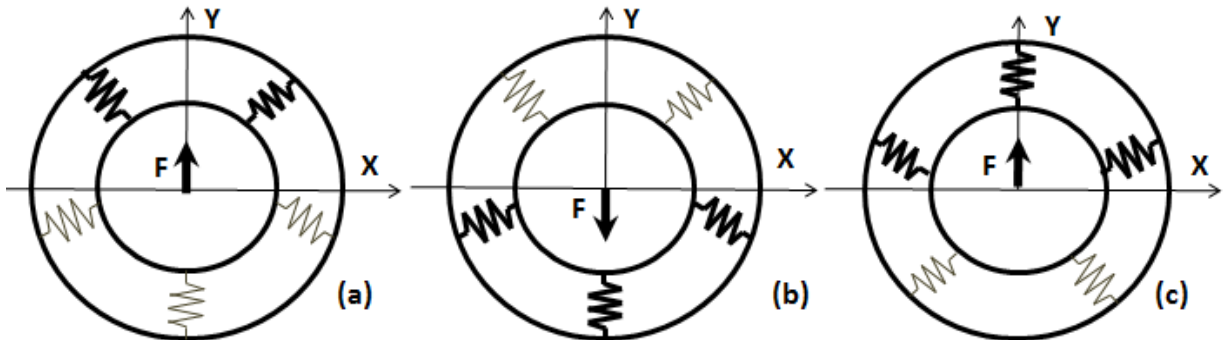


Figure 2: Angular variation of (a) Direct Stiffness and (b) Cross coupled stiffness; taken from [6]

$$[K(t)] = \begin{bmatrix} K_{11} & K_{12} \\ K_{21} & K_{22} \end{bmatrix} = \begin{bmatrix} K_{xx} - K \sin(n\omega t) & K_{xy} \cos(n\omega t) \\ K_{yx} \sin(n\omega t) & K_{yy} + K \cos(n\omega t) \end{bmatrix} \quad (2)$$

Here  $K_{xx}$  and  $K_{yy}$  are the mean values of stiffness variation along  $x$  and  $y$  directions respectively,  $K$  is the amplitude of variation of direct stiffness.  $K_{xy}$  and  $K_{yx}$  are the amplitudes of cross coupled stiffness variation. The shortcoming of this analysis by Srinath et. al. [6] was that loads were applied only in the positive direction to calculate the stiffness values. In reality, the stiffness obtained will be different when the loads are applied in the negative direction. This asymmetric nature of stiffness is not captured in Eq. (2) and needs to be determined. From Eq. (2), when force is applied in positive  $y$  direction as shown in Fig. 3(a) at time  $t$ , the direct stiffness  $K_{22}$  is  $K_{yy} + K \cos(n\omega t)$ . However on applying force in negative  $y$  direction at the same instant  $K_{22}$  should change because the number of active springs in the load zone changes as shown in Fig. 3(b). But it can be observed from Fig. 3(c) that applying force in negative  $y$  direction at the same instant is equivalent to applying force in positive  $y$  direction when the bearing has rotated by an additional angle of  $\pi$ , which would take time equal to  $\pi/\omega$ . Hence the value of  $K_{22}$  changes as per Eq. (3) when force is applied in negative  $y$  direction.


 Figure 3: Load applied in (a) Positive  $y$  direction (b) Negative  $y$  direction (c) Positive  $y$  direction for a  $180^\circ$  rotated configuration. Active springs that transfer the load in load zone are shown in thick colour.

$$K_{22} = K_{yy} + K \cos\left(n\omega\left(t + \frac{\pi}{\omega}\right)\right) = K_{yy} - K \cos(n\omega t) \quad (3)$$

Thus we see that the direct stiffness in  $y$  direction changes its sign depending upon the direction of force or displacement response. The same analogy applies to cross coupled stiffness as well. It should be noted that the sign changes because  $n$  is an odd number. The asymmetry does not arise if  $n$  is even. This asymmetric nature of bearing stiffness makes the vibration analysis complicated because we now have to account for different bearing stiffness depending upon the displacement response. Equations (4)-(7) correspond to expressions for the stiffness parameters depending on the sign of displacement response.

$$K_{11} = \begin{cases} K_{xx} - K \sin(n\omega t), & x > 0 \\ K_{xx} + K \sin(n\omega t), & x < 0 \end{cases} \quad (4)$$

$$K_{12} = \begin{cases} K_{xy} \cos(n\omega t), & y > 0 \\ -K_{xy} \cos(n\omega t), & y < 0 \end{cases} \quad (5)$$

$$K_{21} = \begin{cases} K_{yx} \sin(n\omega t), & x > 0 \\ -K_{yx} \sin(n\omega t), & x < 0 \end{cases} \quad (6)$$

$$K_{22} = \begin{cases} K_{yy} + K \cos(n\omega t), & y > 0 \\ K_{yy} - K \cos(n\omega t), & y < 0 \end{cases} \quad (7)$$

Considering that  $K_{xx} = K_{yy}$  and  $K_{xy} = K_{yx}$ , and substituting the value of  $[K(t)]$ , Eq. (1) can be simplified and non-dimensionalized to two dimensional coupled asymmetric Mathieu equation as Eqs. (8) and (9). The non-dimensional parameters are defined in Eq. (10).

$$\frac{d^2 x^*}{dt^{*2}} + [\delta \mp \varepsilon_1 \sin(2t^*)]x^* \pm [\varepsilon_2 \cos(2t^*)]y^* = 0 \quad (8)$$

$$\frac{d^2 y^*}{dt^{*2}} + [\delta \pm \varepsilon_1 \cos(2t^*)]y^* \pm [\varepsilon_2 \sin(2t^*)]x^* = 0 \quad (9)$$

$$n\omega t = 2t^*; \delta = \frac{4K_{xx}}{mn^2\omega^2}; \varepsilon_1 = \frac{4K}{mn^2\omega^2}; \varepsilon_2 = \frac{4K_{xy}}{mn^2\omega^2}. \quad (10)$$

Where  $m$  is the mass of inner race,  $n$  is the number of rollers and  $\omega$  is the angular speed of rotation. This is a linear, coupled, un-damped and parametric equation of motion. For a given geometry and material of bearing, the only parameter that changes in the equation of motion is the operating speed  $\omega$ . The objective is to predict the speed ranges for which the system turns unstable. This is done by analysing the value of a Lyapunov-like exponent [7]. In the current work we have used the same stiffness parameters as calculated by [6]. The values of stiffness parameters are given in Table 1. The system has five rolling elements ( $n = 5$ ) and mass ( $m$ ) of unity.

Table 1 : Stiffness values and Bearing data

Attributes	Values	Stiffness parameter	Mean value (N/m)	1 <sup>st</sup> harmonic (N/m)
Bore diameter	20 mm	$K_{xx}$	$5 \times 10^8$	$24 \times 10^6$
Outer diameter	47 mm	$K_{yy}$	$5 \times 10^8$	$24 \times 10^6$
Width	14 mm	$K_{xy}$ or $K_{yx}$	0	$60 \times 10^6$

### 3. Lyapunov-like exponent

A system is said to be stable if the amplitude of its vibration does not grow exponentially with time. For simple systems, stability can be numerically verified by plotting displacement vs time and checking if the amplitude shoots up with time. A more scientific approach to check stability of systems governed by asymmetric Mathieu equations was proposed by Marathe et. al. [7]. They formulated a parameter called Lyapunov-like exponent whose value can indicate the stability or instability of the system. Their work however was confined to single degree of freedom systems such as an inverted pendulum with asymmetric elastic restraints.

Since governing equations of motion Eqs. (8) and (9), are in two variables namely  $x$  and  $y$ , a four dimensional phase space can be defined whose four axes correspond to  $x, \dot{x}, y$  and  $\dot{y}$ . To calculate the Lyapunov-like exponent, time evolution of a vector in this four dimensional phase space is studied. This is done by making use of Matlab ordinary differential equation solver ODE45 which makes use of Runge-Kutta method to numerically solve for the equation. By employing a more efficient computational approach which involves passing vectorized arguments to the ODE solver, we

extended the concept of Lyapunov-like exponent from single DOF system to the case of 2-DOF coupled asymmetric Mathieu equations. The in-built Matlab routine for implementing event detection algorithm was used to correctly estimate the sign changes occurring in the stiffness terms.

A random initial unit vector  $\vec{V}_1(t)$  is defined at time  $t = 0$ . The non-dimensionalized equation has a time period  $T = \pi$ . Hence the unit vector is evolved in first iteration from time  $t = 0$  to  $t = \pi$ . Thus the vector  $\vec{V}_1$  becomes  $\vec{V}_1(\pi)$  by the end of first iteration. Let  $N_1$  be the Euclidean norm of the vector  $\vec{V}_1$  after first iteration, that is  $N_1 = \|\vec{V}_1(\pi)\|$ . Now the initial vector for the second iteration  $\vec{V}_2(0)$  is defined as  $\vec{V}_2(0) = \frac{\vec{V}_1(\pi)}{\|\vec{V}_1(\pi)\|} = \frac{\vec{V}_1(\pi)}{N_1}$ . After second iteration  $N_2$  will be the norm of the vector  $\vec{V}_2(\pi)$ . Thus the Lyapunov-like exponent is defined after numerically evaluating the norm for sufficient number of iterations. If  $p$  iterations are carried out, then Lyapunov-like exponent  $L$  is defined as Eq. (11).

$$L = \frac{1}{(p-50)} \sum_{i=51}^p \log(N_i) \tag{11}$$

Here for calculating the Lyapunov-like exponent, only the values starting from 51<sup>st</sup> iteration are taken in order to avoid the initial transient effects. The system is stable if the value of  $L$  is negative and unstable if it is positive. Figure 4 shows the time history of solutions for the Eqs. (8) and (9) for particular values of  $\delta$ ,  $\epsilon_1$  and  $\epsilon_2$ . Figures 4(a) and 4(b) correspond to stable  $\delta$ ,  $\epsilon_1$  and  $\epsilon_2$  values since the amplitude of vibration in x and y directions are bounded and the value of Lyapunov-like exponent is negative. Figures 4(c) and 4(d) corresponds to unstable  $\delta$ ,  $\epsilon_1$  and  $\epsilon_2$  values since the amplitude of vibration grows unbounded with time and a positive value is obtained for the Lyapunov-like exponent.

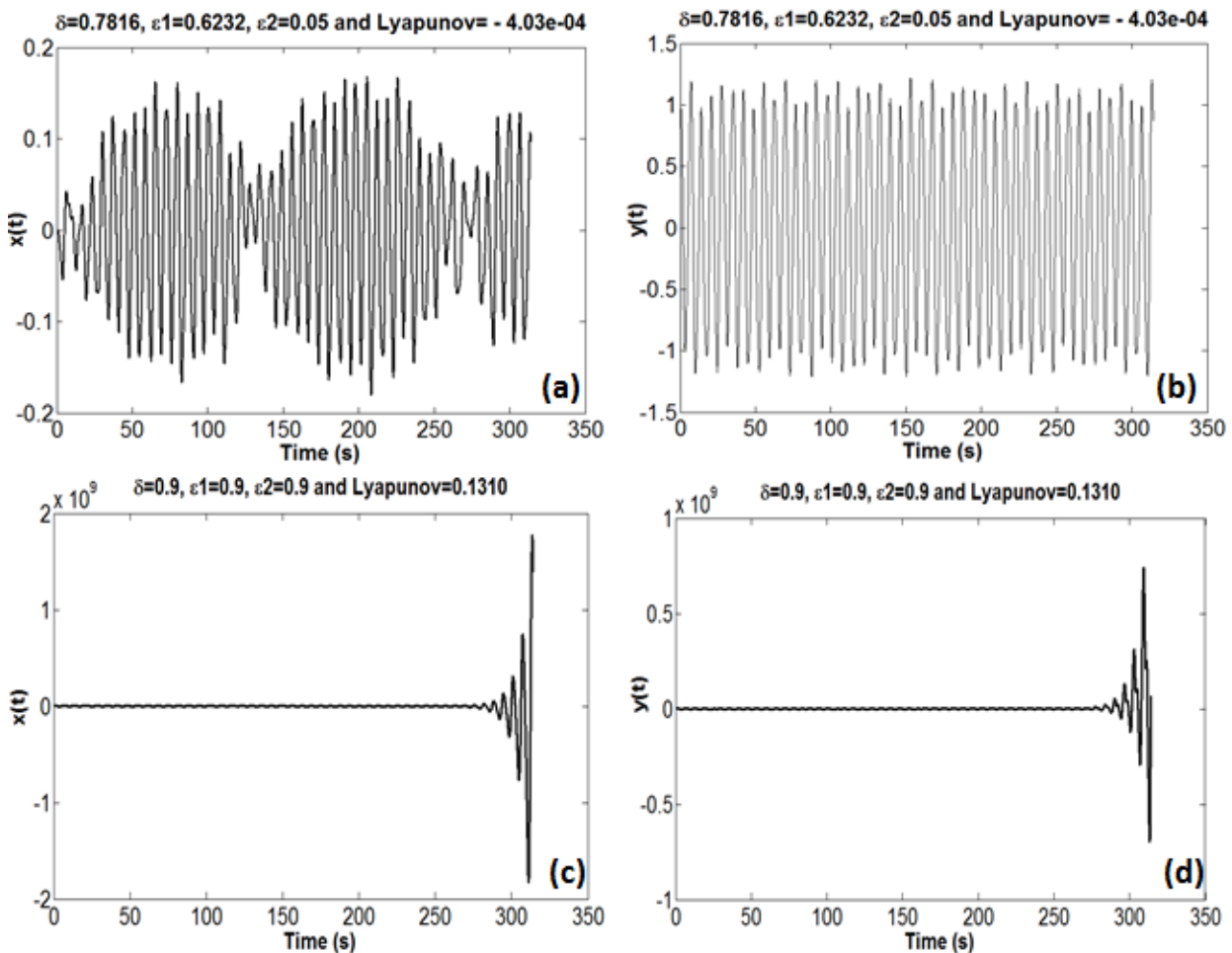


Figure 4: Time history of vibration (a) along x for stable system (b) along y for stable system (c) along x for unstable system (d) along y for unstable system

Since  $\delta, \varepsilon_1$  and  $\varepsilon_2$  are the three parameters that accounts for the parametric excitation, a three dimensional stability lobe plot can be created for a given range of  $\delta, \varepsilon_1$  and  $\varepsilon_2$  values by calculating Lyapunov-like exponent corresponding to each  $(\delta, \varepsilon_1, \varepsilon_2)$  triplet. Unlike the case of a particular bearing configuration with varying rotational speed, these 3-D plots with  $(\delta, \varepsilon_1, \varepsilon_2)$  as the three axes will provide the unstable regions of operation for any given bearing configuration. However, it is difficult to represent the three dimensional stability lobe plot and infer data from it. A two dimensional plot of one of the planes ( $\varepsilon_2=0.05$ ) of the  $(\delta, \varepsilon_1, \varepsilon_2)$  space is shown in Fig. 5. The black regions correspond to unstable parametric values and white regions correspond to stable parametric values. A dense 500×500 grid of points of  $(\delta, \varepsilon_1)$  pairs were taken for plotting the same. In the Matlab ODE solver ODE45, if the arguments are passed sequentially as done in [7], computation would span over a week for obtaining a fine two dimensional grid of Lyapunov-like exponent values. Vectorisation of arguments to ODE45 enabled the evaluation of Lyapunov-like exponents corresponding to all 250,000  $(\delta, \varepsilon_1)$  pairs in a matter of hours. The fractals of instability appearing within major stability regions point out that suggesting a safe range of operational speeds for a particular bearing configuration is challenging.

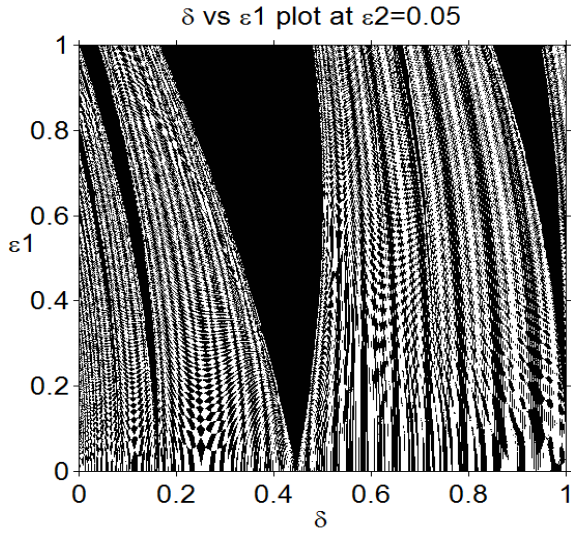


Figure 5: Stability lobe plot for 2-D plane of the  $(\delta, \varepsilon_1, \varepsilon_2)$  space without damping

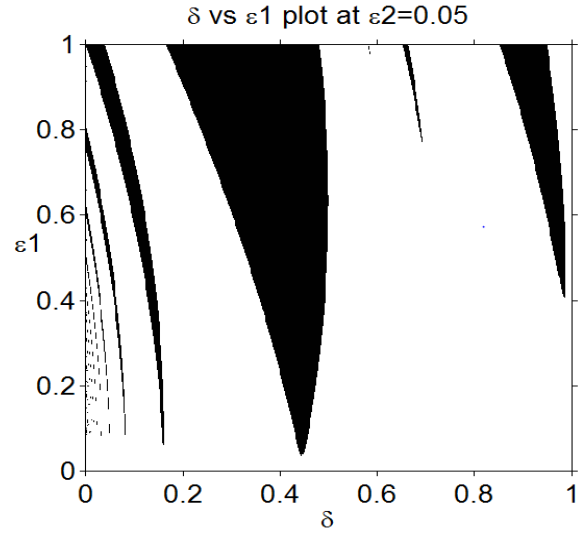


Figure 6: Stability lobe plot for the system in presence of damping

The presence of damping makes this system more stable. When damping effects are taken in to consideration, the governing equations of motion get modified as Eqs. (12) and (13) in the non-dimensionalized form.

$$\frac{d^2x^*}{dt^{*2}} + \hat{C}^* \frac{dx^*}{dt^*} + [\delta \mp \varepsilon_1 \sin(2t^*)]x^* \pm [\varepsilon_2 \cos(2t^*)]y^* = 0 \quad (12)$$

$$\frac{d^2y^*}{dt^{*2}} + \hat{C}^* \frac{dy^*}{dt^*} + [\delta \pm \varepsilon_1 \cos(2t^*)]y^* \pm [\varepsilon_2 \sin(2t^*)]x^* = 0 \quad (13)$$

Where  $\hat{C}^* = \frac{2\hat{C}}{m\omega}$ .  $\hat{C}$  is the damping coefficient. Figure 6 shows the stability lobe plot generated with  $\hat{C}$  taken to be 1% of the value of critical damping  $C_c$ . It can be observed that most of the small instability fractals disappear for such a small percentage of damping and only the major instability lobes remain. This suggests that in real bearing operation conditions where damping is present, only the major instability regions cause unstable vibrations, and it is possible to attain continuous ranges of operational speeds where the system is stable. But it must be emphasized that when bearing operational parameters come within the major instability lobes, parametric vibration with large ampli-

tude occurs and the system becomes unstable. Hence such speeds are definitely to be avoided for safe operation. This is illustrated in the next section.

#### 4. Results

A 3-D plot which shows the value of Lyapunov-like exponent for each  $(\delta, \epsilon_1, \epsilon_2)$  triplet can help in identifying the unstable operational speeds for any bearing. But it is computationally very costly to calculate Lyapunov-like exponent for all  $(\delta, \epsilon_1, \epsilon_2)$  triplets. Here we calculate Lyapunov-like exponent and determine the unstable operational speed range for the particular bearing given in Table 1. The variation of  $(\delta, \epsilon_1, \epsilon_2)$  as per bearing specifications is dictated by Eq. (10). Values of  $\delta, \epsilon_1$  and  $\epsilon_2$  varies as the inverse of  $\omega^2$  when mass, stiffness and number of rollers are fixed. Thus  $\omega$  (rotational speed) is the only parameter that is responsible for the variation of  $(\delta, \epsilon_1, \epsilon_2)$  when only a single bearing assembly is considered. Hence to determine instability of a bearing over a speed range, we calculate  $(\delta, \epsilon_1, \epsilon_2)$  for each  $\omega$  and then calculate the corresponding Lyapunov-like exponent. The value of Lyapunov-like exponent determines if the system is unstable for that lar  $\omega$ . Hence a plot of Lyapunov-like exponent against  $\omega$  can represent the unstable operational speeds. Such a plot is shown in Fig. 7.

For generating Fig. 7, a range of  $\omega$  values from 10 rad/s to 50,000 rad/s was taken in steps of 20 rad/s. Whenever there is a major peak in Fig.7, it denotes a major instability region over that range of  $\omega$ . Table 2 lists the unsafe range of operational speeds corresponding to the major instability peaks of Fig. 7.

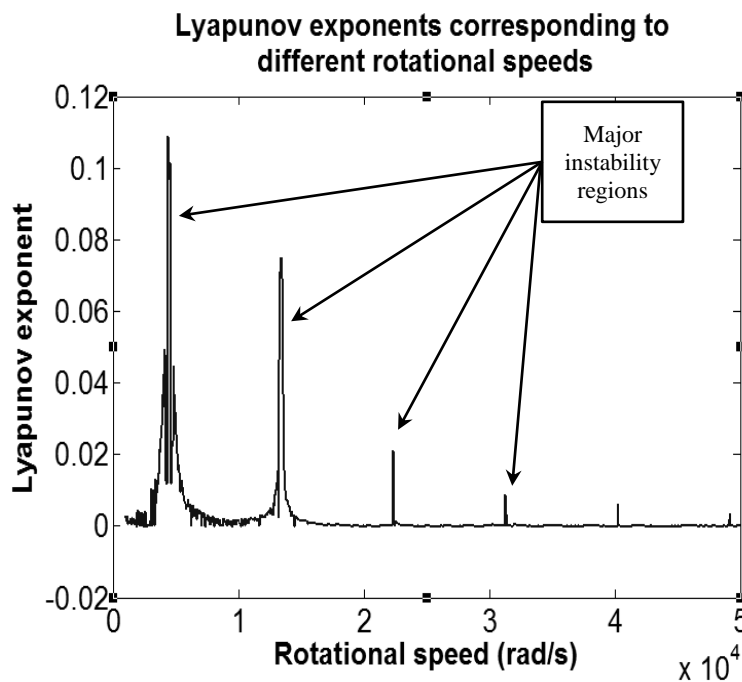


Figure 7: Variation of Lyapunov-like exponent with rotational speed

Table 2: Major instability regions in the absence of damping

Major instability regions	Unsafe operational speed range (rad/s)
1	3100-5650
2	12950-13800
3	22300-22400
4	31300-31400

## 5. Conclusion

In the present work, stability analysis of roller element bearing system is done when parametric excitation is present and the motion of the system is governed by coupled asymmetric Mathieu equation. The asymmetry effect of stiffness values in rolling element bearings was evaluated and governing equations were formulated. Time evolution of magnitude of a unit vector in four dimensional phase space was evaluated numerically using Matlab ODE solver ODE45. A Lyapunov-like exponent defined as the summation of normalized magnitudes of such unit vectors after sufficient number of iterations was taken as the indicator of instability. The effect of damping on the stability of system was demonstrated using a stability lobe plot where it was observed that the instability fractals disappeared even for a damping value equal to 1% that of critical damping. This suggests that in a real bearing operation where damping is present, a continuous range of safe operational speeds can be obtained. A particular bearing configuration was chosen and Lyapunov-like exponents for a range of values of rotational speeds were calculated to suggest the operational speeds which are definitely unsafe in terms of parametric vibration.

The study has been conducted for a specific bearing configuration, but the formulation developed can predict the unstable speed ranges for any rolling element bearing if the mass and stiffness values of the bearing are known. This can aid a bearing manufacturer in cross-checking whether their specified speed ranges for a bearing are coherent with stable vibration regions. This becomes an immediate industrial application of the work.

## REFERENCES

1. Aktürk N., Uneeb M. and Gohar R., The effects of number of balls and preload on vibrations associated with ball bearings, *J. Tribol* **119(4)**, 747-753, (1997).
2. Walters C. T., The dynamics of ball bearings. *ASME Journal of Lubrication Technology*, **93**, 1–10, (1971).
3. Gupta P. K., Dynamics of rolling element bearings Parts I-IV. *ASME Journal of Lubrication Technology*, **101**, 293–326, (1979).
4. Shimizu H. and Tamura H., Vibration of rotor based on ball bearing. 3rd report: static stiffness of a ball bearings containing a large number of balls, *Bull. Jap. Soc. Mech. Engrs.*, **11**, 825–837, (1968).
5. Nayfeh A. H and Mook D. T., *Nonlinear Oscillations*, John Wiley and Sons, New York, (1995).
6. Srinath R., Sarkar A. and Sekhar A. S., Parametrically excited vibration in rolling element bearings, *Inter noise, Melbourne*, (2014).
7. Marathe A. and Chatterjee A., Asymmetric Mathieu equations, *Proc. R. Soc. A*, **462**, 1643–1659, (2006).